Journal of Microencapsulation, 2011; 28(8): 771–782

ISSN 0265-2048 print/ISSN 1464-5246 online
DOI: 10.3109/02652048.2011.621552

informa
healthcare

Biofriendly bonding processes for nanoporous implantable SU-8 microcapsules for encapsulated cell therapy

Krishnamurthy Nemani[1], Joonbum Kwon[2], Krutarth Trivedi[2], Walter Hu[2], Jeong-Bong Lee[2] and Barjor Gimi[1,2,3]

[1]*Department of Radiology, Dartmouth Medical School, Hanover, NH, USA,* [2]*Department of Electrical Engineering, University of Texas at Dallas, Richardson, TX, USA, and* [3]*Department of Medicine, Dartmouth Medical School, Hanover, NH, USA*

Abstract

Mechanically robust, cell encapsulating microdevices fabricated using photolithographic methods can lead to more efficient immunoisolation in comparison to cell encapsulating hydrogels. There is a need to develop adhesive bonding methods which can seal such microdevices under physiologically friendly conditions. We report the bonding of SU-8 based substrates through (i) magnetic self assembly, (ii) using medical grade photocured adhesive and (iii) moisture and photochemical cured polymerization. Magnetic self-assembly, carried out in biofriendly aqueous buffers, provides weak bonding not suitable for long term applications. Moisture cured bonding of covalently modified SU-8 substrates, based on silanol condensation, resulted in weak and inconsistent bonding. Photocured bonding using a medical grade adhesive and of acrylate modified substrates provided stable bonding. Of the methods evaluated, photocured adhesion provided the strongest and most stable adhesion.

Keywords: nanoporous microcapsules, magnetic self-assembly, photocured adhesion, SU-8 surface modification, biofriendly molecular bonding

Introduction

Cells from non-human sources can be grafted in humans to restore functional deficiencies. These cells are often entrapped in hydrogel microbeads to prevent immune rejection of the graft (Figure 1(a)). The hydrogel provides a physical barrier between the host's immune molecules (large molecules) and the graft, while small pores in the hydrogel allow the exchange of nutrients, ions, gases and other small molecules that are essential for the survival and the effective functioning of the graft. However, these hydrogels are tortuously organized polymers that cannot guarantee impenetrability to immune molecules (Iwata et al., 1994; Shoichet et al., 1996).

Alternately, non-human cells can be encapsulated in microcapsules of imperviable material. Extremely precise pores or channels on the surfaces of these microcapsules can guarantee impenetrability to immune molecules while allowing the exchange of essential small molecules (Figure 1(b)). We have outlined a strategy, and attendant processes, to fabricate such nanoporous microcapsules using SU-8 (Gimi et al., 2009a, b; Kwon et al., 2009) which is an epoxy-based, biocompatible polymer (Kotzar et al., 2002; Voskerician et al., 2003; Cho et al., 2008). Each microcapsule comprises a hollow cuboid base that contains the therapeutic cells, and a nanoporous lid that closes the microcapsule (Figure 1(b)).

To transition this cell encapsulation technology to the clinic, it is imperative to seal the microcapsule's base and lid using a biofriendly approach. This bonding should be non-toxic to the encapsulated cells and to the host. The bonding process criteria include (i) physiologically tolerable temperatures, (ii) physiologically tolerable pH and (iii) stability of the bond in aqueous environments. Most current approaches to adhesively bond SU-8 surfaces do not favour cell survival because they involve high

Address for correspondence: Barjor Gimi, Biomedical NMR Research Center, Dartmouth Medical School, 354W Borwell, DHMC, One Medical Center Drive, Lebanon, NH 03756. USA. Tel: (603) 650-3925. Fax: (603) 650-1717. E-mail: Barjor.Gimi@dartmouth.edu

(Received 10 Mar 2011; accepted 29 Aug 2011)
http://www.informahealthcare.com/mnc

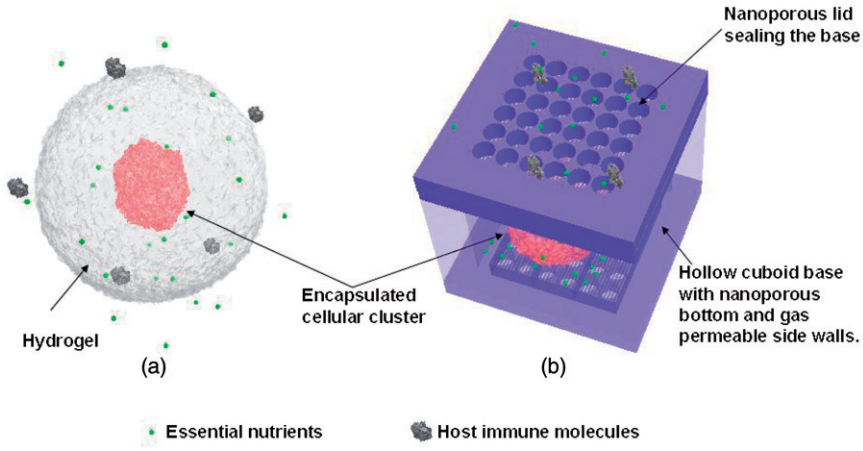

Figure 1. Schematic representation of cellular clusters encapsulated in (a) porous hydrogel which is permeable to small molecules such as essential nutrients, ions and gases and (b) polymeric microcapsule comprising of a nanoporous lid and a hollow cuboid base with gas permeable sidewalls.

temperature, high pressure or oxygen plasma treatment (Yu et al., 2006; Lee and Chung, 2009; Ouellet et al., 2010). Therefore, here we report on biofriendly approaches to seal cell-containing microcapsules that are fabricated using SU-8.

We describe binding SU-8 surfaces based on (1) magnetic force driven self assembly, (2) moisture-cured adhesion of alkoxysilane-modified SU-8 surfaces, (3) photocured adhesion of acrylate-modified SU-8 surfaces and (4) photocured adhesion using a medical grade acrylated urethane based adhesive. Although our current focus is on SU-8 bonding for encapsulated cell therapy, these bonding processes may have broad applicability in sealing SU-8 devices for implantation and for other biomedical applications, as well as in electronics and optics applications that require wet-phase bonding.

Materials

SU-8 and SU-8 developer were procured from Microchem Inc. (www.microchem.com). Sulfuric acid, isopropanol, toluidine blue, rhodamine B, 3-aminopropyltriethoxysilane (APTES), 3-glycidyloxypropyltrimethoxysilane (GPTMS), polyethyleneimine (PEI), triethylamine, toluene, dipentaerythritol pentaacrylate (DPEPA), camphorquinone, triethanolamine, N-vinylpyrollidone and polyethyleneglycol diacrylate were obtained from Sigma-Aldrich Co. (www.sigmaaldrich.com). Trimethoxysilylpropyl-modified-polyethyleneimine (TMSPEI) was procured from Gelest Inc. (www.gelest.com). FM 4–64 was procured from Invitrogen (www.invitrogen.com). Dymax 1161-M adhesive was obtained from Dymax Corporation (www.dymax.com).

Methods

Fabrication of magnetically assembled SU-8 microcapsules

Arrays of hollow cuboid bases and lids of the microcapsule were fabricated separately. Once the bases were filled with their cellular payload, the base and lid structures were assembled using magnetic forces (Figure 2).

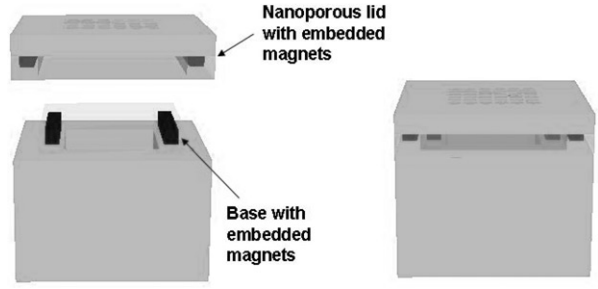

Figure 2. Magnetic assembly of base and nanoporous lid. The base and the lid contain embedded magnets which can facilitate self-assembly of the device.

Base fabrication: The base comprised two discrete components – a *bottom structure* and a *top structure* (Figure 3(a)).

The *bottom structure* of the base was fabricated as follows. The fabrication sequence is summarized in Figure 4. First, 50 μm thick SU-8 was spun on a wafer and patterned to form the bottom face of the cuboid microcapsule. This layer was not photodeveloped to ensure uniform thickness of the next layer. Next, 200 μm thick SU-8 was spun, patterned and baked to form the four side walls of the cuboid.

The *top structure* of the base embedded a permanent magnet in an SU-8 mold to aid in the magnetic assembly of the microcapsule and was fabricated as follows. First, 25 μm thick SU-8 was patterned to form the bottom face of the mold. Then a Cr layer was evaporated on it to promote adhesion, on which a gold layer was evaporated to form a seed layer for electroplating. Next, 40 μm thick SU-8 was spun, baked and patterned to form the side walls of the mold, with a trench in them. CoNiMnP was electroplated in this trench to build the permanent magnets. Finally, 30 μm thick biocompatible SU-8 was patterned to cover the permanent magnets.

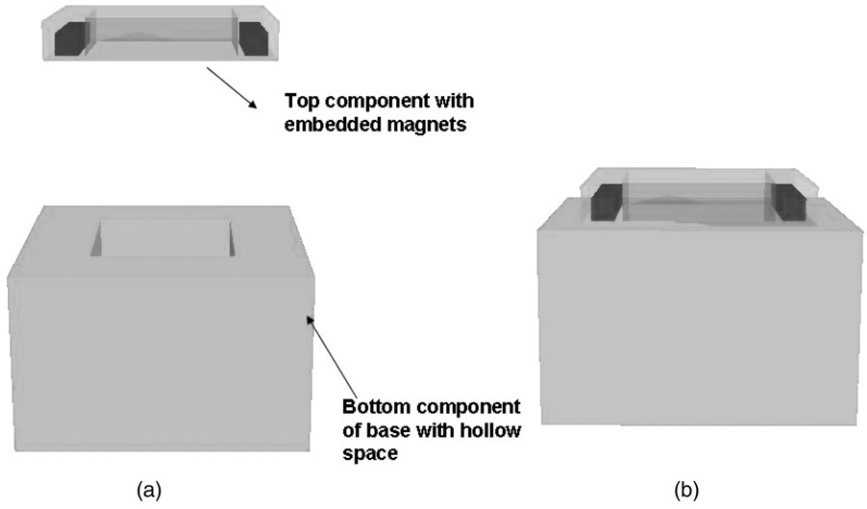

Figure 3. (a) Schematic representation of magnet embedded base comprising of bottom part with the encapsulation volume and a top part comprising of two rectangular magnets embedded in SU-8; (b) the base structure is formed by pressure driven adhesion of the two components using a nanoindentor.

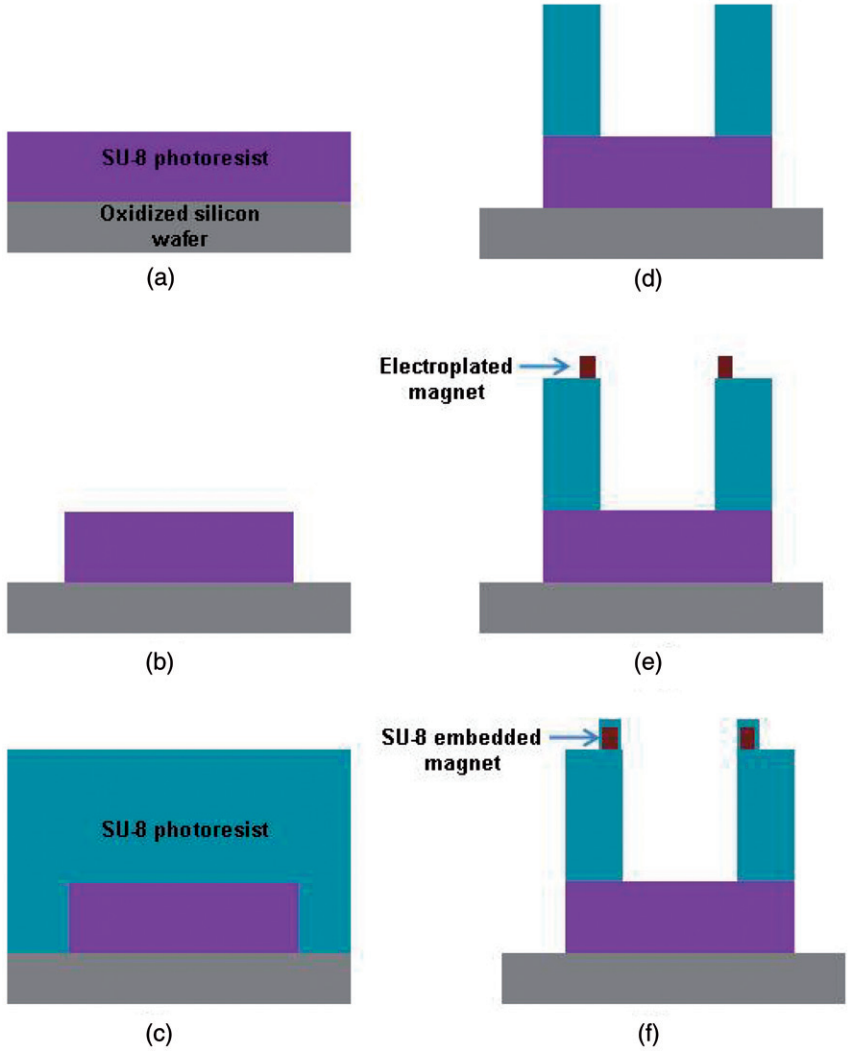

Figure 4. Fabrication process of electromagnet embedded hollow cuboid base: (a) spin coating of 50 μm thick SU-8 layer on an oxidized silicon wafer; (b) patterning of bottom face; (c) spin coating of 200 μm thick SU-8; (d) patterning of the four sidewalls of the base; (e) electroplating of CoNiMnP magnets; (f) patterning of 30 μm thick SU-8 to embed the magnets.

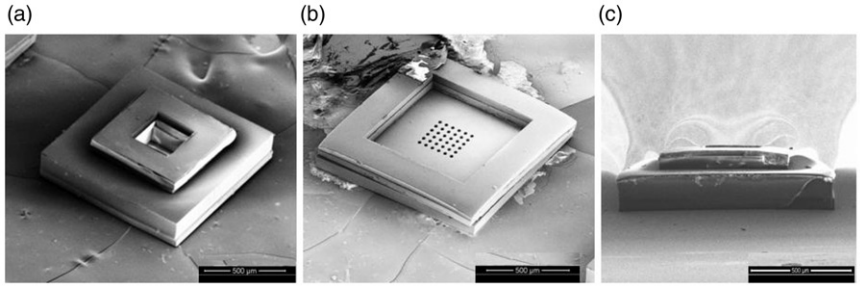

Figure 5. Scanning electron microscope (SEM) image of the base (a) and lid (b). The two discrete components of the base and lid were bonded together using a nanoimprinter. (c) A front-view SEM image betrays contours that indicate that the embedded magnets result in field distortions as expected.

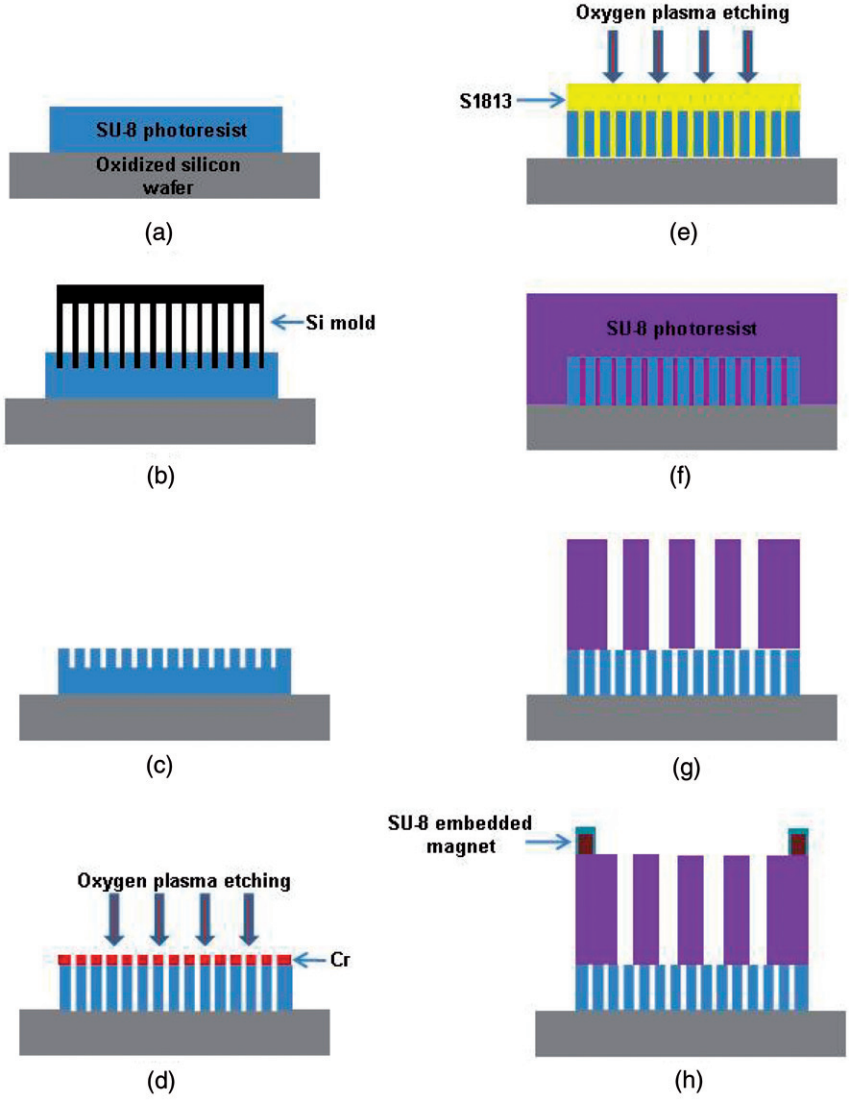

Figure 6. Fabrication process of the magnet embedded nanoporous lid: (a) spin coating of 350 nm thick SU-8 layer on an oxidized silicon wafer; (b) silicon mold imprinting; (c) nanochannel imprint on SU-8 membrane; (d) nanochannel formation by Cr deposition and oxygen plasma etching; (e) patterning of square patterns by S1813 deposition and etching of uncovered SU-8; (f) spin coating of 100 μm thick SU-8; (g) pattering of circular trench array; (h) electroplating of CoNiMnP magnets and embedding them in SU-8.

The *bottom* and *top* structures of the base were aligned and bound at 10 bar and 20°C for 20 min using an Obducat nanoimprinter (Figure 3(b)) and imaged using scanning electron microscopy (SEM; Figure 5(a)).

Lid fabrication: Similar to the base, the lid comprised two discrete components – a *bottom structure* and a *top structure*. The fabrication sequence is summarized in Figure 6.

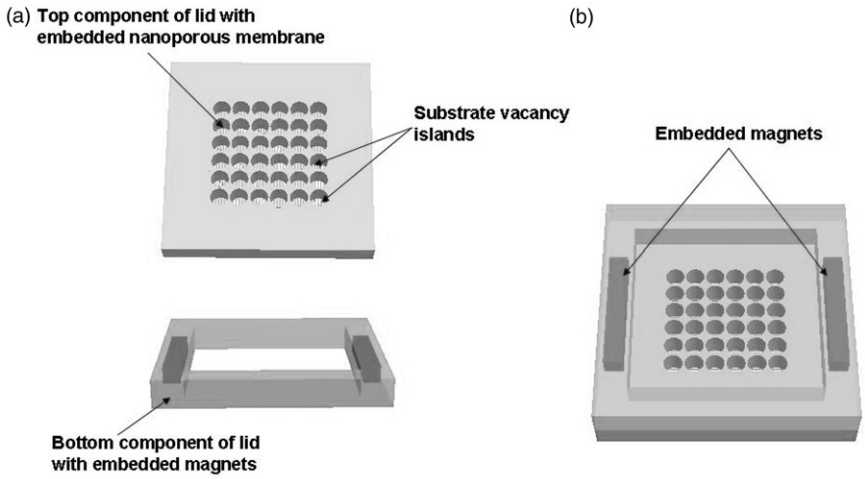

Figure 7. Schematic representation of nanoporous lid with embedded magnets: (a) the lid comprises a top component consisting of a nanoporous membrane supported by a thick SU-8 layer with substrate vacancy islands and a bottom component with embedded magnets; (b) the two components are bound together using a nanoimprinter.

The *top structure* of the lid (Figure 7(a)) was fabricated as follows. First, rectangular nanochannels were formed on a 350 nm thin SU-8 layer using nanoimprinting as detailed by us earlier (Gimi et al., 2009c; Kwon et al., 2009). This nanoporous SU-8 membrane was patterned into square structures by spinning, baking and patterning S1813 photoresist. SU-8 uncovered by S1813 was etched using oxygen plasma. To structurally reinforce this thin nanoporous membrane, 100 μm thick SU-8 was spun on it and patterned with 30 μm diameter substrate vacancies to expose the membrane.

The *bottom structure* of the lid (Figure 7(b)) embedded a permanent magnet in an SU-8 mold to aid in the magnetic assembly of the microcapsule and was fabricated using the same process as the top structure of the base. Similarly, the *top* and *bottom* structures of the lid were bound at 10 bar and 20°C for 20 min using a nanoimprinter and imaged using SEM (Figure 5(b)).

Evaluation of small molecule transport and cell survival post encapsulation

To ascertain small molecule transport and the survival of encapsulated cells in the magnetically assembled microcapsules, a mouse pancreatic islet was encapsulated in each of three microcapsules. Magnetically assembled islet-containing microcapsules were incubated in cell culture medium for 48 h, and subsequently with fresh medium supplemented with FM 4–64. FM 4–64 penetration and islet survival was ascertained by visualizing fluorescence in the red channel by confocal microscopy.

Magnetic resonance imaging (MRI) of embedded magnets

A microcapsule base was embedded in agarose gel and imaged using a 7T Varian Unity Inova magnetic resonance spectrometer equipped with a triple axes gradient. Coronal and axial images were acquired using a spin echo sequence with TR = 3 s, TE = 8.5 ms, field of view = 3 cm × 4 cm, slice thickness = 1 mm and acquisition matrix = 128 × 128.

Fabrication of SU-8 pads for chemical bonding

All adhesive bonding strategies were evaluated using 1.25 cm × 1.25 cm SU-8 pads that were 200 μm thick. First, SU-8 2075 was spun at 900 rpm on an Si wafer that had a sacrificial oxide layer. Next, the wafer was pre-baked at 65°C for 10 min followed by 95°C for 40 min. Next, 1.25 cm × 1.25 cm squares were patterned in the SU-8 layer using a photomask and a UV exposure dose of 400 mJ/cm^2. This was followed by a post-exposure bake at 65°C for 10 min and 95°C for 20 min. The wafers were then cooled and developed using SU-8 developer solution. The resultant 1.25 cm × 1.25 cm × 200 μm pads were released from the wafer using buffered oxide etchant.

Bonding with medical grade adhesive

The acrylated urethane-based medical grade photocured adhesive, Dymax 1161-M (www.dymax.com), was used to bond SU-8 pads. 10 μl of Dymax 1161-M was applied to an SU-8 pad, another pad was then brought in contact with it and maintained under the gentle application of pressure. The pads were photocured for 90 sec using a 150 W xenon lamp source with a focused optical guide. Bonding was also effected after pre-wetting the SU-8 pads with PBS, applying Dymax 1161-M to them and photocuring the adhesive. The bound pads were immersed in PBS and evaluated daily for 3 weeks for bond stability in wet phase as previously described. This bonding procedure was repeated using a 1 : 1 dilution of Dymax 1161-M in isopropanol in order to reduce the viscosity of the adhesive, thus bringing the two

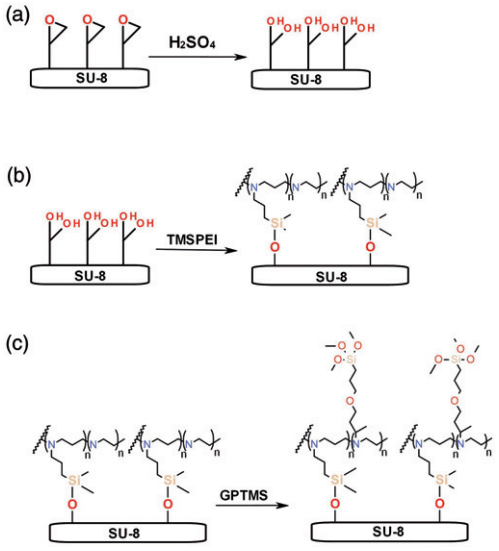

Figure 8. Alkoxysilane modification of SU-8 substrates: (a) hydrolysis of surface epoxy moieties to generate hydroxyl groups and render the surface hydrophilic; (b) formation of a polyethyleneimine layer through a condensation reaction of the hydroxylated surface with trimethoxysilylpropyl-modified-polyethyleneimine (TMSPEI); (c) generation of trimethoxysilane layer on the surface through an epoxy-amine condensation between the amines of PEI and the epoxy group of 3-glycidyloxypropyltrimethoxysilane (GPTMS).

surfaces into closer contact by reducing the thickness of the interfacial adhesive layer. All bonding experiments were performed in triplicate.

Moisture-initiated bonding of alkoxysilane-modified SU-8 pads

Alkoxysilane modification of SU-8 pads was executed in three steps (Figure 8):

1. *Hydroxylation of the SU-8 surface with acid treatment (Figure 8(a))*: Clean SU-8 pads (1.25 cm × 1.25 cm × 200 µm, as detailed above) were treated with 95% H_2SO_4 for 10 s and then immediately bathed in deionized water and soaked for 5 min to remove excess acid. After soaking, the pads were thoroughly washed in deionized water and dried under a stream of nitrogen. Hydroxylation of the SU-8 surfaces was verified by staining with toluidine blue and with rhodamine B, both of which bind to available hydroxyl surface moieties, and by contact angle measurement. For this staining, hydroxylated SU-8 pads were separately incubated in 0.1% (w/v) solution of each dye in phosphate buffer (10 mM, pH = 7.8) for 10 min, then washed in deionized water and dried under a stream of nitrogen. Stained pads were observed under an optical microscope. Contact angles of water droplets on the treated pads were measured using a contact angle goniometer to evaluate the degree of hydrophilicity of acid-treated SU-8. Untreated SU-8 pads were used as controls.
2. *Generation of a polyethyleneimine (PEI) layer on the SU-8 surface (Figure 8(b))*: Acid-hydrolyzed SU-8 pads were incubated with a 10% solution of trimethoxysilylpropyl-modified-polyethyleneimine (TMSPEI) in ethanol and maintained for 12 h at room temperature. Then, the pads were thoroughly washed with ethanol, dried under a stream of nitrogen and cured overnight at room temperature. Surface modification was confirmed by X-ray photoelectron spectroscopy (XPS) and compared against native SU-8, as detailed in the section *''Characterization SU-8 substrate surface modification by X-ray photoelectron spectroscopy (XPS)''*.
3. *Generation of alkoxysilane functionalities on this PEI-modified surface (Figure 8(c))*: The PEI-modified SU-8 pads were incubated for 12 h with a 2% (v/v) solution of 3-glycidyloxypropyltrimethoxysilane (GPTMS) in dry toluene which contained 5% (v/v) triethylamine as a catalyst. Then the pads were serially washed with toluene, ethanol and water. Modification was confirmed by XPS, as detailed in the section *''Characterization SU-8 substrate surface modification by X-ray photoelectron spectroscopy (XPS)''*.

Six pairs of alkoxysilane-modified SU-8 pads were wetted with PBS and maintained in contact at 37°C for 4 h. Bonding was verified by pulling the pads with tweezers. The pads were then further cured overnight. Long term bond stability in aqueous phase was ascertained by immersing the bound pads in PBS for 3 months.

Photoinitiated bonding of acrylate-modified SU-8 pads

Acrylate modification of SU-8 pads was executed in three steps (Figure 9):

1. *Hydroxylation of the SU-8 surface with acid treatment (Figure 9(a))*: SU-8 pads were acid hydrolyzed as described in the previous section.
2. *Generation of aminosilane surface moieties with 3-aminopropyltriethoxysilane (APTES) treatment (Figure 9(b))*: Acid-hydrolyzed SU-8 pads were incubated with a 2% (v/v) solution of APTES in isopropanol for 90 min at room temperature, serially washed with isopropanol and deionized water, dried under a stream of nitrogen and cured overnight at room temperature. This modification was followed by contact angle measurements to evaluate the hydrophilicity of APTES-modified SU-8 and XPS (see the section *''Characterization SU-8 substrate surface modification by X-ray photoelectron spectroscopy (XPS)''*).
3. *Grafting multiple acrylate monolayers to increase the density of surface acrylate moieties (Figure 9(c))*: APTES-modified SU-8 surfaces were incubated with a 20% (v/v) ethanolic solution of dipentaerythritol

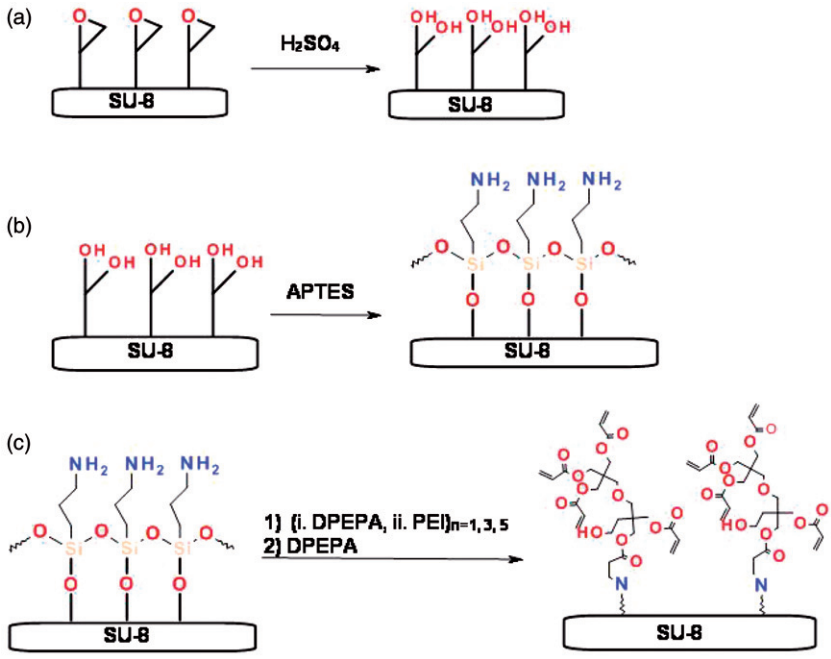

Figure 9. Acrylate modification of SU-8 substrates: (a) hydrolysis of epoxy moieties to generate surface hydroxyl groups; (b) conversion of surface hydroxyls to amine moieties using 3-aminopropyltriethoxysilane (APTES); (c) sequential addition of dipentaerythritol pentaacrylate (DPEPA) and polyethyleneimine (PEI; 1, 3 and 5 cycles) with a final reaction with DPEPA resulting in the formation of acrylate modified SU-8 (2, 4 and 6) layers.

pentaacrylate (DPEPA) for 60 min. The excess reagent was removed by thoroughly rinsing the SU-8 pads with ethanol. The pads were then incubated with PEI in ethanol (1 mg/ml) for 60 min, followed by an ethanol wash to remove excess PEI. These steps were repeated to increase the density of surface acrylate moieties; test pads were prepared with 2, 4 and 6 cycles of this procedure. Then, the SU-8 pads were rinsed with ethanol, dried under a stream of nitrogen and stored under vacuum protected from light. SU-8 pads, modified with 2, 4 and 6 layers of DPEPA, were stained with crystal violet (0.1% v/v aqueous solution) for 15 min to determine the extent of conversion of the acid treated SU-8 surfaces. Stained SU-8 pads were washed with water and dried under a stream of nitrogen. The optical transparency of stained pads at 550 nm was measured. Acid-treated SU-8 pads were used as controls. Acrylate modification was also verified by XPS (see the section *''Characterization SU-8 substrate surface modification by X-ray photoelectron spectroscopy (XPS)''*).

Two acrylate-modified SU-8 pads were bound together through the photopolymerization of surface acrylate moieties. The photoinitiator solution comprised camphorquinone (5 mg), triethanolamine (5 µl), N-vinylpyrollidone (40 µl) in 1 ml PBS. 10 µl of the photoinitiator was applied to one acrylate-modified SU-8 pad and brought into contact with another acrylate modified SU-8 pad. The two surfaces were pressed together between glass coverslips and photocured for 30 min using a fiber optic illuminator that was equipped with a 450 W Halogen lamp and with optical waveguides. Following photocuring, the SU-8 pads were pulled apart with tweezers to test adhesion. This was followed by immersion in PBS and the bond stability was tested daily over a period of 3 weeks. Bonding was also performed by applying 10 µl of the photoinitiator solution to one acrylate modified pad and 10 µl of DPEPA (20% v/v in ethanol) to the other pad.

DPEPA, is a viscous liquid that is immiscible in PBS, which results in the formation of an inhomogeneous interfacial adhesive layer upon photopolymerization. The interfacial layer is characterized by voids which can facilitate the entry of large molecules, thereby negating the selective porosity of the nanoporous lid. Therefore, we used water-soluble polyethyleneglycol diacrylate with the photoinitiator to bind two SU-8 pads with acrylate-modified surfaces. The bound pads were immersed in PBS and the bond strength was tested daily over a period of 3 weeks. All photocured bonding methods were evaluated on three pairs of acrylate modified SU-8 pads to ensure reproducibility.

Characterization SU-8 substrate surface modification by X-ray photoelectron spectroscopy (XPS)

Surface modification was characterized by XPS using an AXIS HS X-ray photoelectron spectrophotometer (Kratos Analytical, USA) with a monochromatic Mg Kα small spot source (1253.6 eV), a multichannel detector and a hemispherical analyzer to measure the binding energies of the emitted photoelectrons. Data was acquired at 1 eV intervals at a pass energy of 160 eV and an acquisition time of 200 ms for each channel. Two spots per sample were analysed and

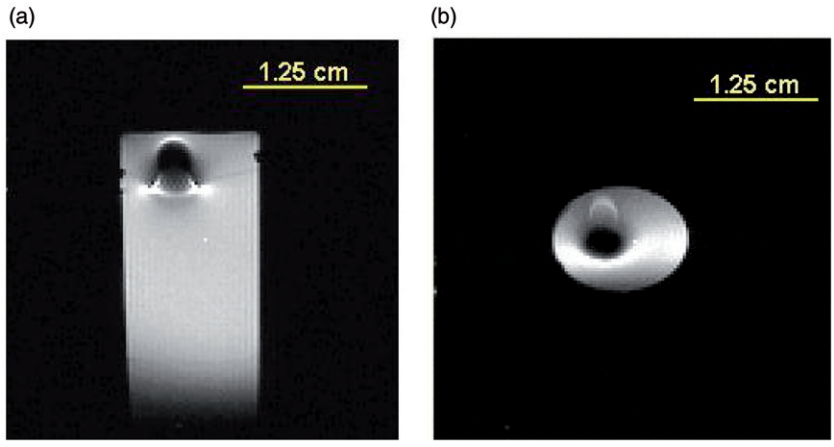

Figure 10. (a) Coronal and (b) axial spin echo magnetic resonance images of a magnet-embedded microcapsule base in an agarose gel phantom.

averaged. Spectra were quantified by manufacturer supplied software.

Results and discussion

Our MEMS-based strategy resulted in the successful fabrication of magnetically assembled, biocompatible, cell encapsulating microcapsules. We successfully bonded two discrete SU-8 components using a nanoimprinter (Figure 5).

The magnetic assembly of the base and the lid can be carried out at room temperature with the components immersed in biofriendly aqueous buffers. This facilitates the sealing of the device in the presence of cellular payload. However, the adhesive strength obtained from our current configuration is not suitable for long term bonding of base and lid. Assuming the two embedded magnets to be two cylindrical magnets, the effective magnetic force of attraction can be calculated based on the equation (Vokoun et al., 2009)

$$F = \left[\frac{K_d A^2}{2\pi}\right]\left[\frac{1}{X^2} + \frac{1}{(X+2L)^2} - \frac{2}{(X+L)^2}\right]$$

$$K_d = \left[\frac{\mu_0 M^2}{2}\right]$$

$$B_0 = [\mu_0 M]$$

where B_0 ($0.17 \sim 0.19$ T) is the magnetic flux density of the embedded CoNiMnP electromagnets (Cho et al., 2000), A ($1000\,\mu m \times 50\,\mu m$) is the area of the magnet, L ($100\,\mu m$) is the length of each magnet, $\times(50\,\mu m)$ is the distance of separation between the two magnets, K_d is the magnetostatic energy density, M is the magnetization and μ_0 is the permeability in vacuum. The calculated force of attraction between the two embedded CoNiMnP electromagnets ($100\,\mu m \times 1000\,\mu m \times 50\,\mu m$) separated by $50\,\mu m$ layer of SU-8 is $1.5 \sim 1.87$ mN (equivalent to an adhesive strength of $\sim$35 kPa). The force of adhesion is much weaker than commercial adhesives and is not suitable for permanent bonding. However, the approach may have utility in bonding devices embedded with larger magnets combined with magnetic material of higher magnetization.

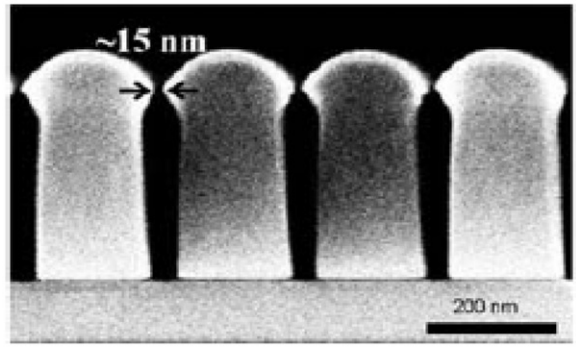

Figure 11. Cross-sectional scanning electron micrograph of the nanoporous membrane. The highly reproducible 15 nm pore size facilitates the selective filtration of large molecules and allows the diffusion of small molecules. Figure modified and reproduced with kind permission from Kwon et al. (2009). Copyright American Vacuum Society.

MRI of the magnet-embedded microcapsule confirmed that the permanent magnets were appropriately electroplated in SU-8 (Figure 10). The distortion pattern observed is consistent with susceptibility effects attributable to ferromagnetism and can be a powerful tool in characterizing the embedded magnets and in locating implants (Beuf et al., 1996; Hopper et al., 2006; Gimi et al., 2007). Note the difference in distortion between the axial image and the coronal image owing to the radial asymmetry of the magnet.

The nanoimprinting method described here resulted in a dense array of rectangular nanopores in the surface of our microcontainers with a 15 nm pore width (Figure 11). The nanoporous lid permitted the transport of the small molecule FM 4–64 (Figure 12) which indicates the potential for cell survival. The nanoporous lid should therefore be effective in allowing the transport of nutrients, oxygen and hormones. These nanopores can be fine tuned to effectively exclude large molecules of the immune system while still permitting the transport of nutrients to the graft and cellular products from the graft to the host. Our strategy can be adapted to release other biotherapeutic molecules and drugs *in vivo*.

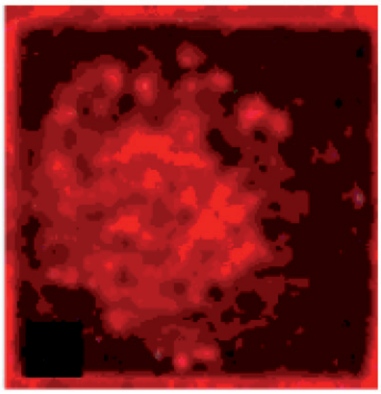

Figure 12. Confocal fluorescence image acquired in the red channel indicating the uptake of the small molecule fluorescence dye FM 4–64 by a pancreatic islet encapsulated in the magnetically self-assembled device. This confirms the efficacy of the nanoporous membrane in small molecule transport. Reproduced with kind permission from Kwon et al. (2009). Copyright American Vacuum Society.

Encapsulated pancreatic islets survived for the 48 h post encapsulation observation period and could be visualized within the optically transparent microcapsules (Gimi et al., 2009c). We are currently performing long term studies of islet survival, function and immunoisolation post-encapsulation.

Bonding with medical grade adhesive

The medical grade adhesive, Dymax 1161-M, resulted in the excellent bonding of SU-8 pads following photocuring. Pre-wetted SU-8 pads also bound to each other. These bonds were stable in wet phase for 3 weeks for every experimental condition described here. Diluting Dymax 1161-M in isopropanol resulted in more uniform surface spreading of the adhesive without adversely affecting binding. Such dilution may result in enhanced surface contact between the substrates of interest which in turn may enhance bond strength.

Characterization of surface modification by X-ray photoelectron spectroscopy (XPS)

The XPS spectra of native SU-8 substrate display two prominent peaks corresponding to the C 1s (282 eV) and O 1s (529 eV) electrons, with an O/C ratio of 0.33 (Figure 13(a)). On acid hydrolysis and subsequent modification with APTES, additional peaks corresponding to N 1s (400 eV) and Si 2p (103 eV), confirming the presence of APTES, were observed with an increased O/C ratio (0.64; Figure 13(b)). This increase is attributable to the increased oxygen atom density on the surface resulting from acid hydrolysis and surface modification with APTES. The Si/N ratio was 0.98, which is consistent with the molecular structure of APTES (Si/N = 1). Further modification of the APTES-coated SU-8 substrate, with multiple layers of PEI and DPEPA, resulted in a spectrum without detectable N and Si peaks (Figure 13(c)), attributed to the heterogeneity of the layers and the surface sensitivity of the technique (i.e. the technique penetration does not allow for observing the Si moieties that reside more than a few nanometers below the surface). The O/C ratio was 0.44 which is consistent with the elemental composition of DPEPA (O/C = 0.48). TMSPEI modification of SU-8 displays the N 1s peak (396 eV) in addition to the C 1s (282 eV) and O 1s (528 eV) peaks (Figure 13(d)). The O/C ratio was 0.24 which is expectedly lower than that of APTES. The formation of TMSPEI layer is further confirmed by the enhanced percentage contribution of N (14.89%) as compared to APTES (7.17%). Incubation of the TMSPEI-modified SU-8 with GPTMS resulted in the formation of a methoxysilane terminated layer. The Si/C and Si/O ratios were 0.12 and 0.17 (Figure 13(e)), respectively, consistent with the molecular structure of GPTMS (Si/C = 0.11, Si/O = 0.2).

Moisture-initiated bonding of alkoxysilane-modified SU-8 pads

Owing to the chemically inert nature of SU-8, we activated its surface prior to chemical modification. Specifically, we opened residual surface epoxy groups to generate hydroxyl moieties using acid hydrolysis. This was confirmed with toluidine blue and rhodamine B staining – acid treated SU-8 pads stained positive for each stain, indicating that the primary amine group of each stain bound to the reactive hydroxyl moieties on the SU-8 surface. Untreated SU-8 controls did not stain. This SU-8 surface activation was also confirmed with contact angle measurements – acid hydrolysis renders the SU-8 surface hydrophilic (Tao et al., 2006); contact angles decrease with increased hydrophilicity. The contact angle was $36^\circ \pm 3^\circ$ for treated SU-8 pads ($n = 3$) and $61^\circ \pm 3^\circ$ for untreated SU-8 ($n = 3$).

PEI surface moieties were generated on SU-8 pads when acid-hydrolyzed pads were incubated with TMSPEI (Figure 8(b)). This was verified by coomassie blue staining of the PEI surface. On subsequent incubation of the pads in the presence of GPTMS, terminal methoxysilane moieties were generated on the SU-8 surfaces. This was confirmed by coomassie blue staining which doesn't bind to the methoxysilane modified surface. Surface modification was further verified by XPS as described in the section "*Characterization of surface modification by X-ray photoelectron spectroscopy (XPS)*".

Moisture initiated hydrolysis of trimethoxysilane groups results in the formation of reactive silanols which can crosslink to bond the surfaces (Figure 14). Weak bonding was observed between the modified SU-8 pads. Of the six pairs tested, one pair of pads exhibited strong binding and could not be peeled apart without breaking the pads after being maintained in PBS for 3 months. Silanol condensation is driven by the expulsion of water which is a product of the reaction. In our attempt to bond the SU-8 substrates in a biofriendly environment, bonding was carried out in the presence of PBS which prevents the removal of water

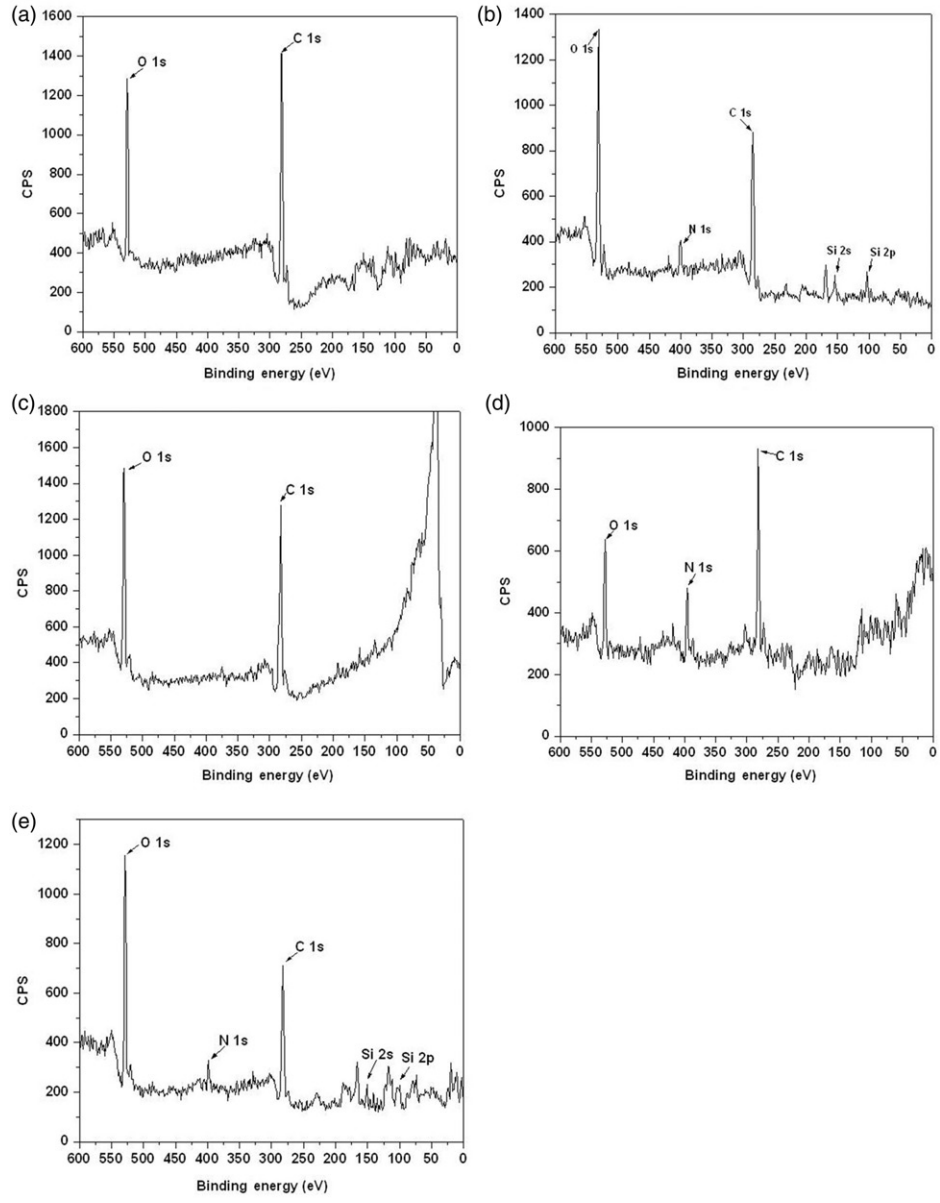

Figure 13. X-ray photoelectron spectra of (a) SU-8 native; (b) APTES modified SU-8 showing additional N 1s, Si 2p and Si 1s peaks; (c) Acrylate modified SU-8 with a C/O ratio comparable to DPEPA; (d) TMSPEI modified SU-8 indicating enhanced N 1s density corresponding to surface grafted PEI; (e) Methoxysilane modified SU-8 confirmed by N 1s, Si 2p and Si 1s peaks in addition to enhanced O density. Chemical modifications of the SU-8 substrates were verified by quantification of the spectral intensities of the C 1s, O 1s, N 1s and Si 2p and Si 1s peaks.

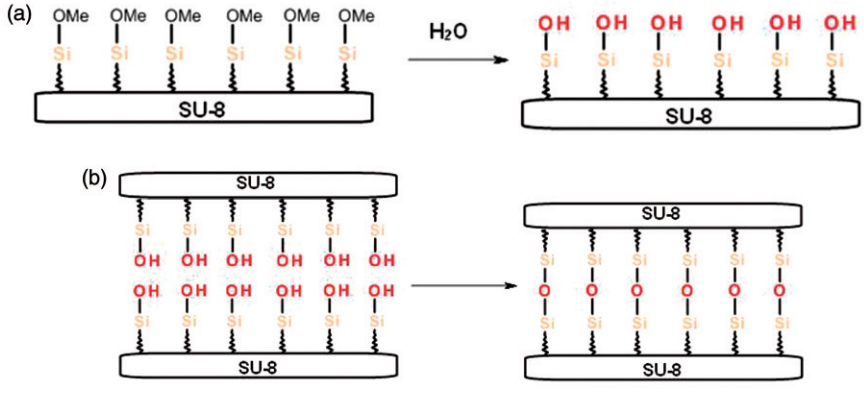

Figure 14. Schematic representation of moisture induced bonding of alkoxysilane modified SU-8 surfaces. (a) Moisture induced hydrolysis of terminal methoxysilane moieties resulting in the generation of reactive silanols. (b) Adhesive bonding of the two surfaces resulting from the silanol bridging between the two surfaces.

during the silanol bridge formation. Though the bonding strategy is efficient in the dry phase (Ouellet et al., 2010), it cannot be applied to bond surfaces in the presence of cells which require constant incubation in culture medium for survival.

Photoinitiated bonding of acrylate-modified SU-8 pads

Acrylate modification of SU-8 pads was carried out following hydroxylation and amino modification of SU-8 using APTES. The amino modification further reduced the water contact angle to $19^\circ \pm 2^\circ$ ($n = 3$). Acrylate modification was verified by crystal violet staining. Crystal violet binds strongly to the acid treated SU-8 substrates and decreases progressively with increasing layers of the acrylate as reflected in the absorbance at 550 nm. Absorbance for hydroxylated SU-8 = 1.15. Absorbance for 2, 4 and 6 layers of acrylate = 0.095, 0.050 and 0.043, respectively. This indicates a higher density of acrylate moieties with repeated cycles of modification. APTES and acrylate modifications were also verified by XPS as described in the section *''Characterization of surface modification by X-ray photoelectron spectroscopy (XPS)''*. Acrylate-modified SU-8 pads showed strong adhesive bonding following photopolymerization. The bound pads could not be pulled apart with tweezers. This bonding was stable with immersion in PBS for 3 weeks, after which the SU-8 pads dissociated. Bonding was attributable to the photopolymerization of surface acrylates, catalyzed by triethanolamine and N-vinylpyrollidone. However, even the highest density of acrylates was insufficient for long term binding SU-8 pads, which required the addition of DPEPA to the photoinitiator. When the photoinitiator solution was supplemented with DPEPA, this bond was stable over 3 months and continues to be stable. The dependence of long term stability on the presence of DPEPA in the photoinitiator solution during polymerization is not conducive to the formation of a homogenous interfacial adhesive layer. As mentioned earlier, DPEPA is a viscous liquid and is immiscible in aqueous buffers, thus disturbing the homogeneity of the photoinitiator solution. Also, the viscosity of the solution increases the interfacial distance between the two surfaces. Use of a water miscible acrylate such as polyethyleneglycol diacrylate can overcome this shortcoming. Stability of bonding in photoinitiator mixtures containing polyethyleneglycol diacrylate are in progress.

The development of a photocured adhesive procedure based on surface modification of SU-8 provides a distinct advantage over commercially available medical grade photocured adhesives. The high viscosity of the adhesives increase the thickness of the interfacial layer. Since, our applications involve bonding substrates of the order of a few hundred microns, it is essential to minimize the interfacial thickness, preferably to molecular dimensions. The use of low viscosity, water miscible acrylates can help achieve this objective.

Conclusion

Magnetic self-assembly with the embedded CoNiMnP magnets is too weak to hold the device together for the intended application. However, the self-assembled device facilitates the survival of cells and effectively allows the diffusion of small molecules. This can be of potential application in larger devices where bigger magnets can be embedded.

Moisture cured adhesion with alkoxysilane modification provides adhesion in the dry phase, though it was not reproducible in the wet phase. Therefore, this method is not suitable for applications involving encapsulation of cells. Photocured adhesion of SU-8 substrates provides stable and strong bonding both with the acrylate modified SU-8 and commercial, medical grade adhesive. The bound substrates were stable for at least 3 weeks when immersed in PBS indicating good moisture resistance. The short lived bonding obtained with acrylate modified SU-8 could be useful in the sealing of implant for short term implantation. Long term bonding required the addition of the acrylate monomer to the photoinitiator solution. The immiscibility of the monomer with aqueous buffers can be overcome with the use of water miscible acrylates. It would be preferable to incorporate the photoinitiator components onto the surface which would enable contact polymerization on exposure to light. This would reduce the interfacial layer thickness providing near conformal contact between the two surfaces.

Declaration of interest

We acknowledge funding from NIH R01 EB007456 and from a Juvenile Diabetes Research Foundation Innovative Grant Award (BG).

References

Beuf O, Briguet A, Lissac M, Davis R. Magnetic resonance imaging for the determination of magnetic susceptibility of materials. J Magn Reson B, 1996;112:111–8.

Cho HJ, Bhansali S, Ahn CH. Electroplated thick permanent magnet arrays with controlled direction of magnetization for MEMS application. J Appl Phys, 2000;87:6340–2.

Cho SH, Lu HM, Cauller L, Romero-Ortega MI, Lee JB, Hughes GA. Biocompatible SU-8-based microprobes for recording neural spike signals from regenerated peripheral nerve fibers. IEEE Sens J, 2008;8:1830–6.

Gimi B, Artemov D, Leong T, Gracias DH, Bhujwalla ZM. MRI of regular-shaped cell-encapsulating polyhedral microcontainers. Magn Reson Med, 2007;58:1283–7.

Gimi B, Kwon J, Kuznetsov A, Vachha B, Magin RL, Philipson LH, Lee JB. A nanoporous, transparent microcontainer for encapsulated islet therapy. J Diabetes Sci Technol, 2009a;3:297–303.

Gimi B, Kwon J, Liu L, Su Y, Nemani K, Trivedi K, Cui Y, Vachha B, Mason R, Hu W, et al. Cell encapsulation and oxygenation in nanoporous microcontainers. Biomed Microdevices, 2009b;11:1205–12.

Gimi B, Kwon J, Trivedi K, Krishnamurthy N, Hu W, Lee J. 2009c. Nanoimprinted, magnetically assembled microcontainers for cell therapy, XVIIth International Conference on Bioencapsulation, Groningen, Netherlands.

Hopper TAJ, Vasilic B, Pope JM, Jones CE, Epstein CL, Song HK, Wehrli FW. Experimental and computational analyses of the effects of slice distortion from a metallic sphere in an MRI phantom. Magn Reson Imaging, 2006;24:1077–85.

Iwata H, Kobayashi K, Takagi T, Oka T, Yang H, Amemiya H, Tsuji T, Ito F. Feasibility of agarose microbeads with xenogeneic islets as a bioartificial pancreas. J Biomed Mater Res, 1994;28:1003–11.

Kotzar G, Freas M, Abel P, Fleischman A, Roy S, Zorman C, Moran JM, Melzak J. Evaluation of MEMS materials of construction for implantable medical devices. Biomaterials, 2002;23:2737–50.

Kwon J, Trivedi K, Krishnamurthy NV, Hu W, Lee J-B, Gimi B. SU-8-based immunoisolative microcontainer with nanoslots defined by nanoimprint lithography. J Vac Sci Technol B, 2009;27: 2795–800.

Lee NY, Chung BH. Novel poly(dimethylsiloxane) bonding strategy via room temperature "chemical gluing". Langmuir, 2009;25:3861–6.

Ouellet E, Yang CWT, Lin T, Yang LL, Lagally ET. Novel carboxyl-amine bonding methods for poly(dimethylsiloxane)-based devices. Langmuir, 2010;26:11609–14.

Shoichet MS, Li RH, White ML, Winn SR. Stability of hydrogels used in cell encapsulation: An in vitro comparison of alginate and agarose. Biotechnol Bioeng, 1996;50:374–81.

Tao SL, Popat K, Desai TA. Off-wafer fabrication and surface modification of asymmetric 3D SU-8 microparticles. Nat Protoc, 2006;1:3153–8.

Vokoun D, Beleggia M, Heller L, Sittner P. Magnetostatic interactions and forces between cylindrical permanent magnets. J Magn Magn Mater, 2009;321:3758–63.

Voskerician G, Shive MS, Shawgo RS, von Recum H, Anderson JM, Cima MJ, Langer R. Biocompatibility and biofouling of MEMS drug delivery devices. Biomaterials, 2003;24:1959–67.

Yu L, Tay FEH, Xu G, Chen B, Avram M, Iliescu C. Adhesive bonding with SU-8 at wafer level for microfluidic devices. J Phys Conf ser, 2006;34:776.